

# Low-reflection photonic-crystal taper for efficient coupling between guide sections of arbitrary widths

A. Talneau\*

*Laboratoire de Photonique et de Nanostructures, Centre National de la Recherche Scientifique,  
Route de Nozay, F-91460 Marcoussis, France*

Ph. Lalanne

*Laboratoire Charles Fabry de l'Institut d'Optique, Centre National de la Recherche, BP 147, F-91403 Orsay, France*

M. Agio\*

*Istituto Nazionale per la Fisica della Materia—Dipartimento di Fisica "A. Volta," Università degli Studi di Pavia,  
Via Bassi 6, I-27100 Pavia, Italy*

C. M. Soukoulis\*

*Research Center of Crete, P.O. Box 1527, GR-71110 Heraklion, Crete*

Received March 22, 2002

We design and fabricate a new taper structure for adiabatic mode transformation in two-dimensional photonic-crystal waveguides patterned into a GaInAsP confining layer. The taper efficiency is validated by measurement of a reduction of the reflection between an access ridge and a photonic-crystal guide with one missing row from 6% to less than 1%. This taper is then incorporated into a 60° bend; simulations demonstrate a 90% transmission between multimode ports. © 2002 Optical Society of America  
OCIS codes: 130.0130, 130.2790.

Photonic-crystal (PC) guiding structures may permit the development of compact and integrated photonic integrated circuits, provided that the guiding structures can achieve low propagation losses and high transmission efficiencies in the different configurations needed in photonic integrated circuits. As many optical functions require various photonic-crystal waveguide (PCW) widths, an adiabatic taper advantageously allows one to optimize independently the PC guiding configuration, e.g., of a bend, a combiner, or a splitter, for coupling to a cavity or a fiber or for laser integration.

Recent advances have pointed out, in the case of PCs patterned into standard semiconductor heterostructures, low losses for wide and thus multimode straight PCWs or coupled resonator optical waveguides.<sup>1,2</sup> It is clear, however, that at a bend such multimode ports lead to mode scrambling, which prevents cascading. We focus in the following on the bend as a meaningful example of the generic issues of photonic integrated circuits. Different approaches to reduce this effect have been attempted,<sup>3–5</sup> but the best fundamental mode transmission is reached for the narrowest line defect (one missing row), as the PCW is monomode in the investigated domain.<sup>6,7</sup> Hence a compromise has to be found, since wide PCWs exhibit low propagation losses but poor bend transmission and narrow PCWs exhibit higher propagation losses but better bend transmission. An overall absolute optimized transmission may be obtained with a wide PCW in the straight sections and a narrower monomode PCW at the bends. An efficient, adiabatic taper channeling power between the fundamental mode of the wide section into the narrow section, before and after the bend, is therefore a prerequisite. Several papers have proposed tapers devoted mainly

to the ridge–PCW transition, but, to our knowledge, none was measured, except the one reported in Ref. 8, which did not rest on guided optics.

The principle of operation of our proposed taper relies on the manufacture of holes with progressively varying diameter and depth.<sup>9</sup> This variation synthesizes an artificial material with a gradient effective index.<sup>10</sup> Calculations performed with a three-dimensional exact electromagnetic theory demonstrated transmission better than 83% on the full PC bandgap.<sup>11</sup> Such a taper has been implemented in PCWs fabricated on a two-dimensional PC consisting of a triangular array (period  $a = 450 \mu\text{m}$ ) of holes drilled on a GaInAsP confining layer. We denote by  $W_n$  the PCW formed by removal of  $n$  rows of air cylinders in the  $\Gamma K$  direction of the PC. All the PCWs are included between ridge-access guides for fiber-to-fiber measurements. The fabrication process is similar to that reported in Refs. 1 and 5. Because of the large mode mismatch between a ridge and a strongly confined  $W_1$  PCW, we first couple the  $1.1\text{-}\mu\text{m}$ -wide ridge-access guide to  $W_3$ ; previous measurements demonstrated that the transmission is  $>97\%$  for a proper ridge width.<sup>1</sup> The tapering from  $W_3$  to  $W_1$  is obtained by a progressive increase in the hole diameters of both inner lines of holes on a 10-row-long PC taper as is visible in the micrograph in Fig. 1. It should be emphasized that reducing the ridge-access width, with the aim of direct coupling to  $W_1$ , will only strangle the mode and increase the losses by coupling to the numerous radiation and lossy modes in the substrate unless the tapered part of the ridge is included within the PCW.<sup>12,13</sup> Such an approach is difficult to implement when the PC is an array of air holes within a semiconductor material, instead of dielectric rods in air.

We first validate the taper efficiency experimentally by measuring the reflected power at the transition when coupling from W3 to W1. For this purpose, we fabricate two different W1s: One W1 is 60 rows long and is directly coupled to the ridge-access guide on both sides; the other one is 120 rows long, with no taper on one side and a taper toward a very short section of W3 (Fig. 1) on the other side. Transmission spectra are measured with a TE-polarized fiber-to-fiber setup in the 1500–1590-nm wavelength domain.<sup>1</sup> A typical transmission spectrum displays a complex structure that we attribute to the beating of the two fringe systems. These systems arise from the two cavities, L1 and L2, formed between the facets and the transition ridge access, W1. We treat the data by Fourier transforming the spectra. Figure 2(a) shows two peaks for the first sample that we unambiguously attribute to cavities L1 and L2. From the knowledge of L1 and L2 cavity lengths, we can deduce a group effective index  $n_g = 3.63$ . Taking into account parameters already evaluated in Refs. 1 and 5, we find that the contrast of each fringe system obtained by filtering the transmission spectrum leads to the same reflectivity,  $R = 6\%$ , for both ridge–W1 transitions. Figure 2(b) shows only one peak for the second sample, which is associated with the nontapered ridge–W1 transition (here L2). Given the noise level, the upper bound of the reflectivity for the taper is below 1%. These PC structures are dry etched with reactive ion etching, and the etch depth is limited to 1  $\mu\text{m}$ .<sup>1,5</sup> The rather low etch depth leads to very high propagation losses in the case of W1 guides, which prevent oscillation of L1 + W1 as well as L2 + W1 and also of the whole L1 + W1 + L2 cavities.

As a second validation of this taper concept, we apply our taper design to a 60° PCW bend with W3 access to combine the advantages of low propagation losses in a broad W3 multimode PCW in the straight sections and of good transmission on the monomode W1 PCW at the bend itself. As long as waveguide W3 is excited in its fundamental mode, this design allows fundamental-to-fundamental mode channeling. The W3 straight PCW is channeled through this taper into a W1 sharp bend and then channeled again out through a second taper on a W3 PCW. By decreasing the radii of the holes that are close to the dielectric channel, it is possible to go continuously from W1 to W3. The W1 dispersion relation changes, and more modes appear until the hybrid W1- $x$  PCW becomes W3. We adopt the notation W1- $x$  to label a hybrid W1 PCW, where the holes close to the dielectric defect have the radius reduced by  $x\%$  of its bulk value, with  $x \in [0, 100]$ . Figure 3 shows the dispersion relation for W1-30% compared with that of a W3 waveguide. The solid (dashed) curves represent the even (odd) modes with respect to the waveguide axis. Although W3 does not exhibit monomode regions, W1-30% is monomode for frequencies 0.251–0.270 (in units of  $c/a$ ). Therefore, it is not necessary to taper down to W1, as W1-30% already exhibits monomode behavior. To design the most compact bend, we eliminated the straight W1-30% sections before and after the bend; this is similar to a W3 bend with a

constriction.<sup>14</sup> The new structure does not guarantee any more fundamental-to-fundamental mode transmission, because the taper is not properly a W1-30% waveguide. Nevertheless, for sufficiently long tapers we expect that the system will be similar to W1-30%; i.e., it is monomode for certain frequencies.

Two-dimensional finite-difference time-domain simulations<sup>15</sup> demonstrate that a high transmission (>90%) fundamental-to-fundamental mode is achieved in the 7-nm wavelength domain. The electric field pattern for a tapered sharp bend connecting to W3 PCWs at  $a/\lambda = 0.2515$  is plotted in Fig. 4. The tapers are eight unit cells long. Propagation on the fundamental mode is clearly visible, with no mode transformation. A larger transmission bandwidth could be reached by use of a more accurate design.<sup>17</sup>

A very efficient design for coupling PCWs has been proposed and measured. The reflected power at a ridge–W1 PCW is reduced to less than 1%. Such a taper allows a 60° bend, with wide W3 PCW ports with transmission into the fundamental mode of better than 90%. Such a design allows cascading. More generally, the concept of artificial material exploited in this taper design can be implemented in any transition from  $W_i$  to  $W_j$  PCWs, whatever the values of  $i$  and  $j$ , as well as for the transition of any PCW to a ridge through a  $W_k$  PCW, as we have shown for W3 PCWs. This design overcomes the recurrent problem

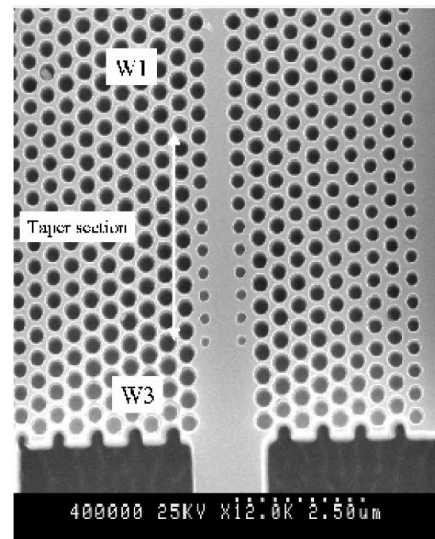


Fig. 1. Scanning electron microscope picture of the tapering section.

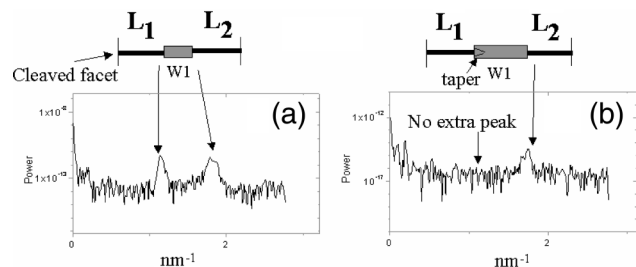


Fig. 2. Fourier-transformed spectra of the transmission spectra through W1 PCW (a) without a taper and (b) with one taper.

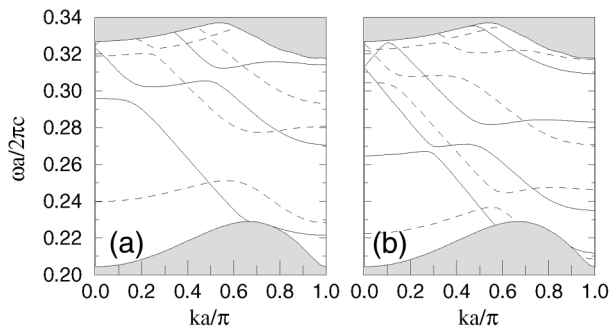


Fig. 3. Dispersion relation for (a) W1-30% PCW and (b) W3 PCW. The solid (dashed) curves refer to even (odd) modes with respect to the waveguide axis. PC parameters:  $\epsilon = 10.5$ ,  $f = 40\%$ , TE polarization. The gray areas represent the bulk PC modes.

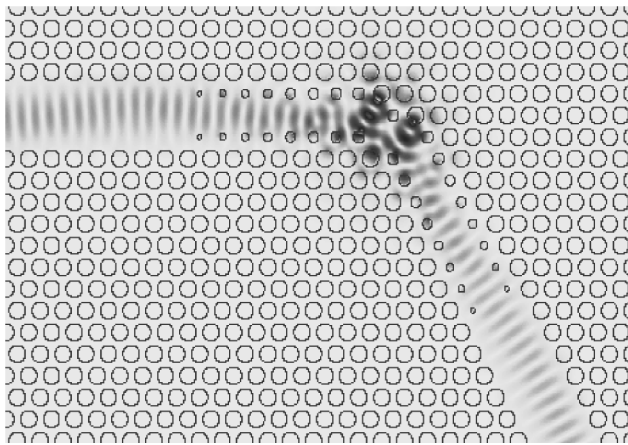


Fig. 4. Electric field through a tapered sharp bend connecting two W3 PCWs. PC parameters:  $\epsilon = 10.5$ ,  $f = 40\%$ , TE polarization,  $a/\lambda = 0.2515$ .

of reflection, which will prevent correct behavior of PC integrated circuits.

M. Agio thanks L. C. Andreani for the development of the FORTRAN subroutines used in the supercell calculation of Fig. 3. Part of this work was supported by the Information Societies Technology program Photonic Crystal Integrated Circuits (contract 1999-11239). A Talneau's e-mail address is anne.talneau@lpn.cnrs.fr.

\*Also with the Ames Laboratory and Department of Physics and Astronomy, Iowa State University, Ames, Iowa 50011.

## References

1. A. Talneau, L. Le Gouezigou, and N. Bouadma, *Opt. Lett.* **26**, 1259 (2001).
2. S. Olivier, C. Smith, M. Rattier, H. Benisty, C. Weisbuch, T. Krauss, R. Houdré, and U. Oesterlé, *Opt. Lett.* **26**, 1019 (2001).
3. S. Olivier, H. Benisty, C. Weisbuch, M. Qiu, A. Karlsson, C. J. M. Smith, R. Houdré, and U. Oesterlé, *Appl. Phys. Lett.* **79**, 2514 (2001).
4. T. Baba, N. Fukaya, and J. Yonekura, *Electron. Lett.* **35**, 654 (1999).
5. A. Talneau, L. Le Gouezigou, N. Bouadma, M. Kafesaki, C. M. Soukoulis, and M. Agio, *Appl. Phys. Lett.* **80**, 547 (2002).
6. M. Lončar, D. Nedeljkovic, T. Doll, J. Vuckovic, A. Schere, and T. P. Pearsall, *Appl. Phys. Lett.* **77**, 1937 (2000).
7. E. Chow, S. Y. Lin, J. R. Wendt, S. G. Johnson, and D. J. Joannopoulos, *Opt. Lett.* **26**, 286 (2001).
8. H. Kosaka, T. Kawashima, A. Tomina, T. Sato, and S. Kawakami, *Appl. Phys. Lett.* **76**, 268 (2000).
9. Ph. Lalanne and A. Talneau, "Structre à cristal photonique pour la conversion de mode," French patent 0115057 (November 21, 2001).
10. M. Palamaru and Ph. Lalanne, *Appl. Phys. Lett.* **78**, 1466 (2001).
11. Ph. Lalanne and A. Talneau, *Opt. Express* **10**, 354 (2002); [www.opticsexpress.org](http://www.opticsexpress.org).
12. A. Mekis, S. Fan, and J. D. Joannopoulos, *J. Lightwave Technol.* **19**, 861 (2001).
13. Y. Xu, R. K. Lee, and A. Yariv, *Opt. Lett.* **25**, 755 (2000).
14. A. Mekis, S. Fan, and J. D. Joannopoulos, *Phys. Rev. B* **58**, 4809 (1998).
15. A. Tavlove, *Computational Electrodynamics: The Finite-Difference Time-Domain Method* (Artech House, Norwood, Mass., 1995).
16. The peak transmission is 95%. The less-than-100% transmission is probably due to the mismatch between the rectangular Finite-difference time-domain mesh and the sixfold symmetry of the PC lattice. The two sections of the PCW are not equivalent in the numerical simulation.
17. A. Chutinan, M. Okano, and S. Noda, *Appl. Phys. Lett.* **80**, 1698 (2002).